IOP PUBLISHING JOURNAL OF PHYSICS D: APPLIED PHYSICS

J. Phys. D: Appl. Phys. **42** (2009) 214008 (8pp) doi:10.1088/0022-3727/42/21/214008

Subcritical crack growth law and its consequences for lifetime statistics and size effect of quasibrittle structures

Jia-Liang Le[1], Zdeněk P Bažant[1] and Martin Z Bazant[2]

[1] Department of Civil and Environmental Engineering, Northwestern University, 2145 Sheridan Road, CEE/A135, Evanston, IL 60208, USA

[2] Department of Chemical Engineering, Massachusetts Institute of Technology, MA 02139, USA

E-mail: z-bazant@northwestern.edu.

Received 16 February 2009, in final form 27 April 2009
Published 22 October 2009
Online at stacks.iop.org/JPhysD/42/214008

Abstract

For brittle failures, the probability distribution of structural strength and lifetime are known to be Weibullian, in which case the knowledge of the mean and standard deviation suffices to determine the loading or time corresponding to a tolerable failure probability such as 10^{-6}. Unfortunately, this is not so for quasibrittle structures, characterized by material inhomogeneities that are not negligible compared with the structure size (as is typical, e.g. for concrete, fibre composites, tough ceramics, rocks and sea ice). For such structures, the distribution of structural strength was shown to vary from almost Gaussian to Weibullian as a function of structure size (and also shape). Here we predict the size dependence of the distribution type for the lifetime of quasibrittle structures. To derive the lifetime statistics from the strength statistics, the subcritical crack growth law is requisite. This empirical law is shown to be justified by fracture mechanics of random crack jumps in the atomic lattice and the condition of equality of the energy dissipation rates calculated on the nano-scale and the macro-scale. The size effect on the lifetime is found to be much stronger than that on the structural strength. The theory is shown to match the experimentally observed systematic deviations of lifetime histograms from the Weibull distribution.

(Some figures in this article are in colour only in the electronic version)

1. Introduction

For many engineering structures, such as bridges, buildings, dams, aircraft and ships, the reliability analysis is of paramount importance because the safety factors guarding against the uncertainties in structural strength are the most uncertain aspect of design. As generally agreed [20, 31, 33], the design must ensure that the failure probability of structure $P_f < 10^{-6}$ for the entire lifetime. Such a small P_f is beyond the means of direct experimental verification by histogram testing. Hence, it is necessary to develop a realistic, physically justified, probabilistic model, which can be verified indirectly.

We restrict attention to the broad class of structures of positive geometry (i.e. structures having a geometry for which the stress intensity factor gradient >0). These structures reach their maximum load and begin softening right after the initiation of a macro-crack from one representative volume element (RVE) of material. When they are brittle, the probability distribution function of structural lifetime is well known. Statistically, the brittle structures are equivalent to the weakest link model in which the number of links, each corresponding to one RVE, is infinite. Noting that the structure survives if and only if all the links (i.e. all RVEs) survive, one can apply the joint probability theorem. In this way one finds that the cumulative distribution functions (cdf) of both the strength and the lifetime of structure must be Weibullian. The distribution type being known, it suffices to calculate or experimentally determine the mean and the standard deviation. Thus the loading or time needed to reach $P_f = 10^{-6}$ is obtained easily. Not so for quasibrittle structures.

The quasibrittle structures consist of brittle heterogeneous, or quasibrittle, materials in which the size of the RVE

(typically about three inhomogeneity sizes) is not negligible compared with the structure size. They include concrete, tough ceramics, fibre composites, rocks, sea ice, snow slabs, wood, etc, and all brittle materials on the micrometre scale. Their salient feature is that, as the structure size increases, the failure behaviour transits from quasi-plastic (characterized by a load-deflection diagram with a yield plateau) to brittle (no plateau but a sudden load drop as soon as the maximum load is reached) [5–8, 15].

Along this transition, spanning about three orders of magnitude of structure size, the strength cdf gradually changes from Gaussian to Weibullian [10, 13, 14]. The consequences for safety are serious because, e.g. when the coefficient of variation of strength is $\omega = 0.1$ (a typical value), the distance from the mean to the point of $P_f = 10^{-6}$ is 4.75ω for the Gaussian cdf, and 6.65ω for the Weibull cdf. This difference is huge and requires a large change of safety factors, which underscores the importance of finding a theoretical basis for the dependence of cdf on the structure size (and shape). A logical basis is the atomistic fracture mechanics.

The atomistic basis of the size effect on the cdf of strength has recently been established [9–11], and the present objective is to do the same for the lifetime. Significant advances in lifetime prediction have already been made for various engineering materials. Tobolsky and Eyring [42] first developed an activation energy model for the lifetime of polymers, and later Zhurkov [46, 47] championed a similar model for the lifetime of polymers, alloys and non-metallic crystals. However, they neglected the effect of restoration of ruptured interatomic bonds during random interatomic crack growth. This restoration was later taken into account by Hsiao *et al* [27], but it was in the context of an atomic pair potential, which is insufficient to capture the near-symmetry of forward and backward jumps during the crack propagation. All of these models led to deterministic results and could not predict the type of lifetime cdf.

Other approaches have been taken to characterize the lifetime statistics for fibrous materials, composites and ceramics [18, 19, 24, 32, 36, 37]. Many of them used some intuitively chosen functions, e.g. the two-parameter Weibull distribution [24, 32], lognormal distribution [1] and Weibull hazard function [18, 19, 36, 37]. However, these functions were not (and could not be) physically justified for quasibrittle structures, and often the histogram fits were poor [24, 32].

To calculate structure lifetime, the rate of creep growth of a subcritical crack must be known. For constant loads, the growth rate has been extensively investigated for decades, both theoretically and experimentally [21–23, 26, 29, 41, 44]. The crack growth rate law was first studied in the context of corrosive environment [26, 44], where the classical rate process theory was adopted to explain the effect of chemical reaction on the crack propagation rate at low stress [25, 26, 44].

For the stress-dominated crack growth, a power-law function has been empirically proposed to describe the dependence of crack growth velocity on the applied stress [21, 22, 41]. Some theoretical justification of the power-law form of crack growth law has recently been suggested [23, 32],

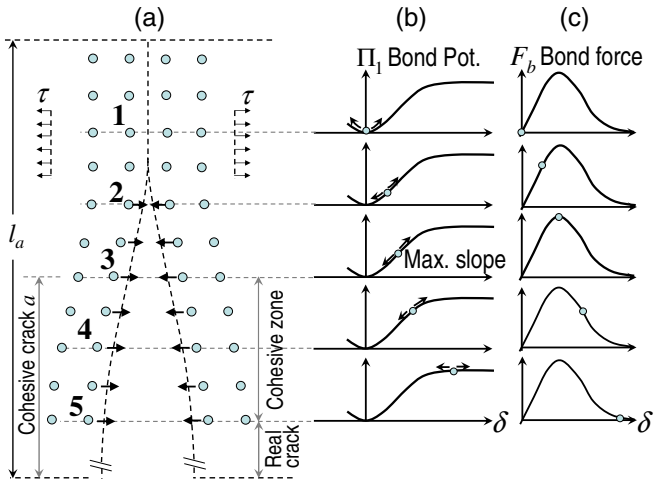

Figure 1. Fracture of atomic lattice block.

based on the break frequency of a bond between a pair of two atoms. Such a justification, however, is problematic, for three reasons: (1) The pair potential, such as the Morse potential, neglects the contribution of surrounding atoms, which is major. (2) As the crack grows, the breakage of each pair occurs not in one step but over a series of many steps separated by metastable states. (3) The scale bridging between the atomic scale and the macro-scale is missing. Thus, the power law for crack growth rate has so far been justified only empirically.

This paper presents a physical justification of the power-law form of crack growth rate based on the atomistic fracture mechanics and on the multiscale transition of the fracture kinetics from nano- to macro-scale. The crack growth law is then used to extend a recently developed theory of the strength distribution of quasibrittle structures to the statistics of structure lifetime under constant load. An extension to other monotonic loading histories would be straightforward and will not be presented here.

2. Crack growth rate at nano-scale

Consider the crack propagation in an atomic lattice block, which is subjected to some remote stress (figure 1(*a*)). On the nano-scale, the propagation of a nano-crack is directly caused by the breaks of atomic bonds ahead of the crack tip. As the crack propagates, the separation between the opposite atoms across the crack, δ, increases by small fractions of their initial distance. The integral of the force transmitted between two opposite atoms, F_b (which includes the contributions of all nearby atoms), is the local potential function $\Pi_1(\delta)$ (figure 1(*b*)), i.e. $F_b(\delta) = \partial\Pi_1(\delta)/\partial\delta$. The bond strength is exhausted at the peak point of the interatomic force-separation curve $F_b(\delta)$ (figure 1(*c*)), which also corresponds to the point of maximum slope of the curve $\Pi_1(\delta)$. This point (labelled 3 in figure 1(*a*)) normally defines the end of the fracture process zone (FPZ), in which the stresses decrease with increasing separation (which is a classical idea of Barenblatt [4]). The FPZ, also called the cohesive zone, begins (and the real crack ends) at the point where the interatomic force is reduced to zero (labelled 5 in figure 1(*a*)).

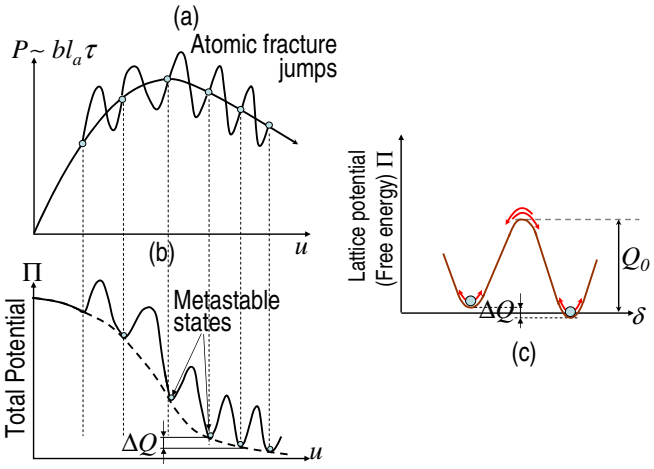

Figure 2. (*a*) Load–displacement curve of atomic lattice block, (*b*) curve of free energy potential of atomic lattice block, (*c*) activation energy barriers of atomic lattice block for fracture extension and shortening.

As the crack propagates through the atomic lattice block, its length changes by jumps equal to the atomic spacing δ_a. During each jump, one barrier on the overall potential Π of the lattice block must be overcome. Therefore, the load–displacement curve of the lattice $P(u)$ exhibits the wavy shape instead of the usual smooth curve (figure 2(*a*)). After each jump, potential Π decreases slightly (figure 2(*b*)). Because of thermal activation, the states of the atomic lattice block fluctuate and can jump over the activation energy barrier in either direction (forward or backward, figure 2(*c*)), though not with the same frequency. When crack length a jumps by one atomic spacing, the activation energy barrier Q changes by a small amount ΔQ corresponding to the energy release by fracture, which is associated with the equilibrium load drop P from one metastable state to the next.

The FPZ of the nano-crack cannot be assumed to be negligible compared with the size of the nano-scale atomic lattice block, l_a. Therefore, the approximation by equivalent linear elastic fracture mechanics (LEFM), in which the tip of an equivalent sharp LEFM crack lies roughly in the middle of the FPZ, needs to be used. We may idealize the crack as planar and three-dimensional, growing in a self-similar manner. Its stress intensity factor can generally be expressed as $K_\mathrm{a} = \tau\sqrt{l_\mathrm{a}}k_\mathrm{a}(\alpha)$ where $\alpha = a/l_\mathrm{a}$ = relative crack length, $k_\mathrm{a}(\alpha)$ = dimensionless stress intensity factor, $\tau = c\sigma$ = remote stress applied on the nano-scale atomic lattice block; c = nano–macro stress concentration factor and σ = macro-scale stress applied to the structure. The corresponding energy release rate function is

$$\mathcal{G}_\mathrm{a}(\alpha) = K_\mathrm{a}^2/E_1 = k_\mathrm{a}^2(\alpha)l_\mathrm{a}\tau^2/E_1, \tag{1}$$

where E_1 = elastic modulus for a continuum approximation of the lattice (which is larger than the macroscopic elastic modulus E). The increment of energy that is released when the crack advances by δ_a along its entire perimeter of length $\gamma_1\alpha l_\mathrm{a}$ is

$$\Delta Q = \delta_\mathrm{a}(\gamma_1\alpha l_\mathrm{a})\mathcal{G}_\mathrm{a} = V_\mathrm{a}(\alpha)\frac{\tau^2}{E_1}, \tag{2}$$

where $V_\mathrm{a}(\alpha) = \delta_\mathrm{a}(\gamma_1\alpha l_\mathrm{a}^2)k_\mathrm{a}^2(\alpha)$ = activation volume (note that if the stress tensor is written as $\tau\boldsymbol{s}$ where τ = stress parameter, one may write $V_\mathrm{a} = \boldsymbol{s} : \boldsymbol{v}_\mathrm{a}$ where $\boldsymbol{v}_\mathrm{a}$ = activation volume tensor, as in the atomistic theories of phase transformations in crystals [2]).

Since each atomic jump δ_a is much shorter than the cohesive crack length, the interatomic separation increases during each jump by only a small fraction of the atomic spacing. So, the activation energy barrier for a forward jump, $Q_0 - \Delta Q/2$, differs very little from the activation energy barrier for a backward jump, $Q_0 + \Delta Q/2$ (Q_0 = activation energy at no stress). Consequently, the jump of the state of atomic lattice block must be happening in both directions, though with slightly different frequencies. Based on the transition rate theory [28, 35], the first-passage time for each transition is given by Kramer's formula [39], according to which the net frequency of crack jumps is [9]

$$f_1 = \nu_\mathrm{T}(\mathrm{e}^{-(Q_0-\Delta Q/2)/kT} - \mathrm{e}^{-(Q_0+\Delta Q/2)/kT}) \tag{3}$$

$$= 2\nu_\mathrm{T}\mathrm{e}^{-Q_0/kT}\sinh[V_\mathrm{a}(\alpha)/V_\mathrm{T}], \tag{4}$$

where $V_\mathrm{T} = 2E_1kT/\tau^2$, ν_T = characteristic attempt frequency for the reversible transition, $\nu_\mathrm{T} = kT/h$ where $h = 6.626 \times 10^{-34}$ J s = Planck constant, T = absolute temperature and k = Boltzmann constant. Considering typical values of the parameters in equation (4), one finds $V_\mathrm{a}/V_\mathrm{T} \ll 1$ [10]. Therefore, equation (4) becomes

$$f_1 = C_\mathrm{T}\tau^2 \tag{5}$$

where $C_\mathrm{T} = \gamma_1\alpha k^2(\alpha)\mathrm{e}^{-Q_0/kT}(\delta_\mathrm{a}l_\mathrm{a}^2/E_1h)$. For the foregoing derivation to be valid, it is also required that $\Delta Q \ll kT \ll Q_0$, or $\tau \ll (E_1kT/V_\mathrm{a})^{1/2}$.

More generally, the growth of nano-crack can be attributed to two mechanisms: (1) stress-driven drift and (2) stress-independent diffusion. The drift velocity caused by applied stress is simply given by

$$v = \delta_\mathrm{a}f_1. \tag{6}$$

When the applied stress becomes low enough, the stress-independent diffusion will govern the crack growth. The rate of nanocrack growth may then be treated as a first-passage process of random walk [38].

Consider, for simplicity, a one-dimensional random walk in which the crack-tip, initially located at x_0, moves at drift velocity v (a multi-dimensional random walk, requiring a numerical approach, would be more realistic but is not needed for our purpose). The occupation probability of the crack tip, $p(x,t)$ (i.e. the probability of the crack tip being at position x at time t), satisfies the Fokker–Plank equation [38]:

$$\frac{\partial p(x,t)}{\partial t} + v\frac{\partial p(x,t)}{\partial x} - D\frac{\partial^2 p(x,t)}{\partial x^2} = 0 \tag{7}$$

where $D = \frac{1}{2}\nu_\mathrm{T}\delta_\mathrm{a}^2\mathrm{e}^{-Q_0/kT}$ = diffusivity.

The relative dominance of stress-driven drift over stress-independent diffusion is measured by the Péclet number, $\mathrm{Pe} = vl_\mathrm{a}/2D = 2(l_\mathrm{a}/\delta_\mathrm{a})(V_\mathrm{a}/V_\mathrm{T})$. The mean time for the crack tip to reach the domain boundary ensues by calculating the flux

of occupation probability at the boundary [38]. A reflecting boundary is considered at $x = 0$, and an absorbing boundary at $x = l_a$. When the crack tip reaches the reflecting boundary, the tip can move only in the positive x direction, i.e. the flux of the occupation probability at $x = 0$ vanishes. When the crack tip reaches the absorbing boundary, the lattice fails, i.e. the occupation probability at $x = l_a$ is zero. By using these boundary conditions and solving equation (7), one obtains the mean exit time or mean failure time as

$$\langle t \rangle = \frac{l_a^2}{2D}\left[\frac{1 - x_0/l_a}{\mathrm{Pe}} + \frac{\cosh \mathrm{Pe}}{(\mathrm{Pe})^2 \mathrm{e}^{\mathrm{Pe}}} - \frac{\cosh(\mathrm{Pe}\, x_0/l_a)}{(\mathrm{Pe})^2\, \mathrm{e}^{\mathrm{Pe}\, x_0/l_a}}\right]. \tag{8}$$

For a small Pe (Pe $\to$ 0), the mean failure time is $l_a^2/2D$. For large Pe, the mean failure time approaches $(l_a - x_0)/v$. It is found that, when Pe > 4, the failure process is predominantly governed by a stress-dependent drift mechanism.

In fracture, the Péclet number is normally large enough such that the stress-independent crack front diffusion is negligible [10]. Therefore, the nano-crack velocity is the stress-driven drift velocity:

$$\dot{a} = \nu_1 \mathrm{e}^{-Q_0/kT} K_a^2 \tag{9}$$

where $\dot{a} = \mathrm{d}a/\mathrm{d}t$, $\nu_1 = \delta_a^2(\gamma_1 \alpha l_a)/E_1 h$ and K_a = stress intensity factor of the atomic lattice block. The stress-independent crack growth driven by diffusion (called the environment-assisted crack growth [29]) is nevertheless important in corrosive environments, not considered here.

3. Multiscale transition of fracture kinetics

On the structure scale, the crack growth rate may be described by a simple empirical law [21, 22, 41]:

$$\dot{a} = A \mathrm{e}^{-Q_0/kT} K^n, \tag{10}$$

where A, n = positive empirical constants, K = stress intensity factor at macro-structure scale and a = length of macro-crack. One may set $K = \sigma\sqrt{D_s} k(\alpha)$, where D_s = structure size, $\alpha = a/D_s$ and $k(\alpha)$ = dimensionless stress intensity factor; see also [15, 16, 22, 32, 41]. Exponent n typically ranges from 10 to 30 [21, 32]. Equations (9) and (10) have different exponents but the same form, except that, unlike A, ν_1 depends on α. However, except near the boundaries, the FPZ does not change significantly as the macro-crack propagates through the structure (which is a central tenet behind the constancy of fracture energy G_f). Therefore, all the different relative crack lengths α in the nano-structure of a FPZ must average out to give a constant A.

To explain the difference in exponents n, consider the multiscale transition of the fracture kinetics from nano-scale to macro-scale. This transition may be expressed by the condition that the rate of energy dissipation of the macro-crack must be equal to the sum of energy dissipation rates of all the active nano-cracks a_i $(i = 1, \ldots, N)$ in the FPZ of the macro-crack. Hence,

$$\mathcal{G}\dot{a} = \sum_{i=1}^{N} \mathcal{G}_i \dot{a}_i, \tag{11}$$

where $\mathcal{G}$ and $\mathcal{G}_i$ denote the energy release rate functions for macro-crack a and nano-crack a_i, respectively. Upon expressing the energy release rate in terms of the stress intensity factor and substituting equation (9) for $\dot{a}_i$, one obtains

$$\dot{a} = \mathrm{e}^{-Q_0/kT} \phi(K) \tag{12}$$

where

$$\phi(K) = \sum_{i=1}^{N} \frac{\nu_i K_i^4 E}{K^2 E_i}, \tag{13}$$

where K_i = stress intensity factor of the atomic lattice block containing nano-crack a_i, E_i = elastic modulus of the atomic lattice and $\nu_i = \delta_a^2(\gamma_1 \alpha_i l_i)/E_i h$. In the context of linear elasticity, one may assume $K_i = \omega_i K$, where ω_i are some constants. Hence, one may re-write equation (13) as

$$\phi(K) = K^2 \sum_{i=1}^{N} \frac{\nu_i \omega_i^4 E}{E_i}. \tag{14}$$

The number of active nano-cracks N in the FPZ of the macro-crack must be estimated in a multiscale framework: the FPZ of a macro-crack contains q_1 meso-cracks, each of which contains a meso-FPZ with q_2 micro-cracks, each of which contains a micro-FPZ with q_3 sub-micro-cracks, and so forth, all the way down to the atomic lattice scale. So, if the multiscaling from macro to nano bridges s scales, the number of nano-cracks contained in the macro-FPZ is $N = \Pi_{\mu=1}^{s} q_\mu$.

On scale μ, the number q_μ of activated cracks within the FPZ of the next higher scale must be a function of the relative stress intensity factor K/K_μ, i.e. $q_\mu = q_\mu(K/K_\mu)$ where K_μ = critical K for cracks of scale μ. It may be expected that function $q_\mu(K/K_\mu)$ increases rapidly with increasing K/K_μ while the ratios in $\phi(K)$ vary far less. Therefore, one may replace E_i, ω_i and ν_i by some effective mean values E_a, ω_a and ν_a:

$$\phi(K) = \nu_a \omega_a^4 (E/E_a) K^2 \prod_{\mu=1}^{s} q_\mu(K/K_\mu). \tag{15}$$

Since there appears to be no characteristic value of K at which the behaviour of $q_\mu(K/K_\mu)$ would qualitatively change, the function $q_\mu(K/K_\mu)$ should be self-similar, i.e. a power law [3], $q_\mu(K/K_\mu) = (K/K_\mu)^r$. Consequently, the function $\phi(K)$ should be a power law as well:

$$\phi(K) = \frac{\nu_a \omega_a^4 E}{E_a(\prod_\mu K_\mu^r)} K^{rs+2}. \tag{16}$$

Setting $rs+2 = n$ and substituting $\phi(K)$ back to equation (12), one thus finally obtains the power law for macro-crack growth.

Equation (12) represents the general form of the growth law of cracks at all the scales, from nano to macro. Note that the Arrhenius form of temperature dependence applies for the crack growth at all the scales. The difference in the crack growth rate at various scales is reflected by the difference in the power exponent s and the values of ω_a and K_μ. When passing from nano to macro, exponent s increases, causing the

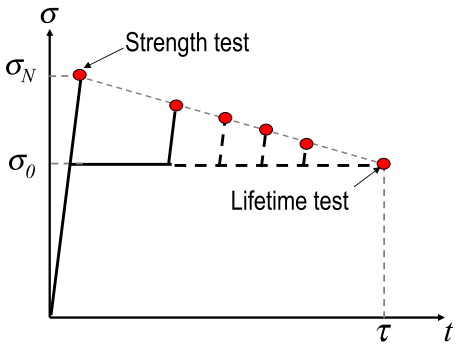

Figure 3. Transition of load histories from strength test to lifetime test.

power-law exponent to increase from 2 at the nano-scale to the experimentally observed values of 10–30 at the macro-scale.

The foregoing analysis shows that, on the nano-scale, the crack growth rate is a power law of exponent 2. Nevertheless, it does not represent a rigorous proof of the power law for macro-crack growth rate. It merely explains physically why the power-law exponent increases on passing to higher scales. Validation by experiments is still essential.

4. Lifetime statistics of quasibrittle structures

The creep crack growth law is important as a link between the strength and lifetime of a RVE. Consider both the strength and lifetime tests for an RVE (figure 3). (1) In the strength test, the load is rapidly increased till the RVE fails. The maximum load registered corresponds to the strength of the RVE, which may be chosen to be equal to σ_N. (2) In the lifetime test, the load is rapidly increased to a certain level σ_0 and then is kept constant till the RVE fails. The load duration up to failure represents the lifetime λ of the RVE at stress σ_0.

Now consider a RVE containing a dominant subcritical crack with initial length a_0. Within the framework of equivalent LEFM, the crack grows to a critical value a_c under some loading history, and then the structure fails by dynamic propagation of the RVE. The stress intensity factor of the RVE can be written as $K = \sigma\sqrt{l_0}k(\alpha_R)$, where $\alpha_R = a_R/l_0$ and a_R = current length of the dominant subcritical crack. Applying the crack growth law for the strength test, one gets

$$\sigma_N^{n+1} = r(n+1)e^{Q_0/kT}\int_{\alpha_0}^{\alpha_c}\frac{d\alpha}{Al_0^{(n-2)/2}k^n(\alpha)}, \qquad (17)$$

where r = loading rate. For the lifetime test, the loading duration λ is usually far longer than the duration of the laboratory strength test. The applied load σ_0 is much lower than the RVE strength, and so the initial increasing portion of the load history makes a negligible contribution compared with the entire loading duration. Thus, by applying the crack growth law for constant load σ_0, one has

$$\sigma_0^n\lambda = e^{Q_0/kT}\int_{\alpha_0}^{\alpha_c}\frac{d\alpha}{Al_0^{(n-2)/2}k^n(\alpha)}. \qquad (18)$$

Comparing equations (17) and (18), one finds that the structural strength and the lifetime are related through the following simple equation:

$$\sigma_N = \beta\sigma_0^{n/(n+1)}\lambda^{1/(n+1)}, \qquad (19)$$

where $\beta = [r(n+1)]^{1/(n+1)}$ = constant.

Recent studies [13, 14] showed that the cdf of RVE strength may be statistically represented by a hierarchical model consisting of bundles (or parallel couplings) of no more than two long sub-chains, each of them consisting of sub-bundles of two or three long sub-sub-chains of sub-sub-bundles, and so on [13, figure 2(e)], until the refinement reaches the nano-scale of atomic lattice, at which the strength distribution has been derived from equation (5) [9, 10]. The hierarchical model indicates that the strength cdf of a RVE can be approximately described to have a Gaussian distribution onto which a Weibull tail (power-law tail) is grafted from the left at a probability of about 10^{-4} to 10^{-3} [14]

$$\text{for } \sigma_N < \sigma_{N,gr} \qquad P_1(\sigma_N) = 1 - e^{-(\sigma_N/s_0)^m}, \qquad (20)$$

$$\text{for } \sigma_N \geqslant \sigma_{N,gr} \qquad P_1(\sigma_N) = P_{gr} + \frac{r_f}{\delta_G\sqrt{2\pi}}\int_{\sigma_{N,gr}}^{\sigma_N} e^{-(\sigma'-\mu_G)^2/2\delta_G^2}\,d\sigma'. \qquad (21)$$

Here σ_N = nominal strength, which is a maximum load parameter of the dimension of stress. In general, $\sigma_N = P_{max}/bD$ or P_{max}/D_s^2 for two- or three-dimensional scaling (P_{max} = maximum load of the structure or parameter of load system, b = structure thickness in the third dimension, D_s = characteristic structure dimension or size). Furthermore, m (Weibull modulus) and s_0 are the shape and scale parameters of the Weibull tail, and μ_G and δ_G are the mean and standard deviation of the Gaussian core if considered extended to $-\infty$; r_f is a scaling parameter required to normalize the grafted cdf such that $P_1(\infty) = 1$ and P_{gr} = grafting probability $= 1 - \exp[-(\sigma_{N,gr}/s_0)^m]$. Finally, continuity of the probability density function at the grafting point requires that $(dP_1/d\sigma_N)|_{\sigma_N^+} = (dP_1/d\sigma_N)|_{\sigma_N^-}$.

Substituting equation (19) into equations (20) and (21), one obtains the lifetime distribution of an RVE:

$$\text{for } \lambda < \lambda_{gr} \qquad P_1(\lambda) = 1 - \exp[-(\lambda/s_\lambda)^{m/(n+1)}] \qquad (22)$$

$$\text{for } \lambda \geqslant \lambda_{gr} \qquad P_1(\lambda) = P_{gr} + \frac{r_f}{\delta_G\sqrt{2\pi}}\int_{\gamma\lambda_{gr}^{1/(n+1)}}^{\gamma\lambda^{1/(n+1)}} e^{-(\lambda'-\mu_G)^2/2\delta_G^2}d\lambda' \qquad (23)$$

where $\gamma = \beta\sigma_0^{n/(n+1)}$ $\lambda_{gr} = \beta^{-1}\sigma_0^{-n}\sigma_{N,gr}^{n+1}$ and $s_\lambda = s_0^{n+1}\beta^{-(n+1)}\sigma_0^{-n}$. Clearly, similar to the cdf of strength, the cdf of lifetime of one RVE has a Weibull tail. The Weibull modulus of this tail is much lower than that of strength distribution. For the same RVE, equations (21) and (23) imply that the grafted probability P_{gr} is the same for the cdfs of both the strength and the lifetime.

For a structure of any size, the RVE must be defined as the smallest material volume whose failure triggers the failure of the structure (of positive geometry). Therefore, the structure may be statistically modelled by a chain of RVEs (weakest link model). It is essential to note that, for quasibrittle materials, the chain must be finite rather than infinite since the RVE size

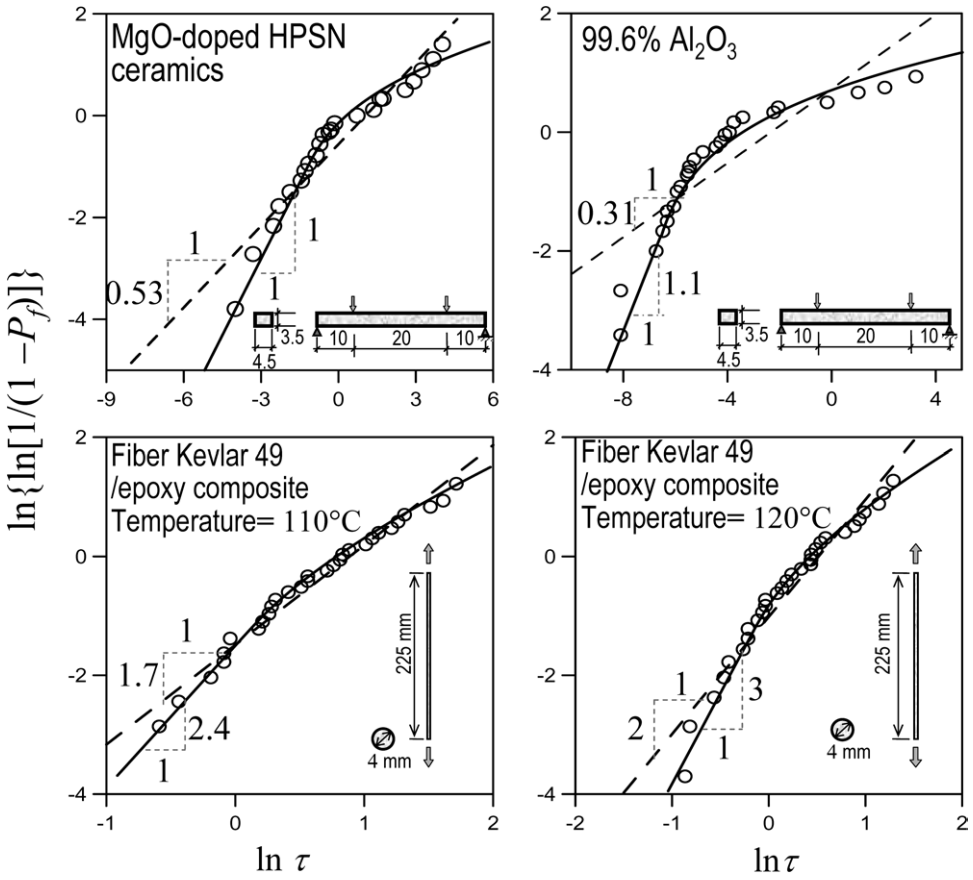

Figure 4. Optimum fits of lifetime histogram of various ceramics and fiber composites (test data from [17, 32]).

is not negligible compared with the structure size. By virtue of the joint probability theorem, the lifetime distribution of a structure subjected to a nominal stress σ_0 can be calculated as

$$P_f(\sigma_0, \lambda) = 1 - \prod_{i=1}^{N} \{1 - P_1[\langle \sigma_0 s(\boldsymbol{x}_i)\rangle, \lambda]\}, \qquad (24)$$

where $\sigma_0 s(\boldsymbol{x}_i)$ = maximum principal stress at the centre of the ith RVE, $s(\boldsymbol{x}_i)$ = the dimensionless stress ratio which represents the stress distribution, $\langle x\rangle = \max(x, 0)$ and σ_0 = nominal stress, which is a parameter of the applied load P having the dimension of stress ($\sigma_0 = c_g P/bD$ for two-dimensional scaling, or $= c_g P/D^2$ for three-dimensional scaling).

For general structures, subdividing the structure into RVEs is to some extent subjective, which may cause some differences in P_f. To avoid such subjective differences, a non-local boundary layer approach has been proposed to evaluate $P_f(\sigma_0, \lambda)$ [10]. As the structure size increases, what matters for the structural failure is the tail of the cdf of lifetime of each RVE: $P_1(\lambda) = (\lambda/s_\lambda)^{\bar{m}}$. Therefore, the lifetime cdf for very large structures must approach the Weibull distribution.

The present analysis (equation (22)) yields a simple general relation between the Weibull moduli of the strength and lifetime distributions, involving the exponent of power law for crack growth rate:

$$\bar{m} = \frac{m}{n+1}. \qquad (25)$$

Identifying Weibull modulus $\bar{m}$ of lifetime distribution by histogram testing is time consuming and costly. Equation (25) makes possible a much more effective determination of $\bar{m}$. To identify $\bar{m}$, one needs only the Weibull modulus of strength distribution, which is best determined by testing the size effect on the mean strength [34], and the exponent of the power law for crack growth rate. The latter can be obtained by standard tests that measure the subcritical crack growth velocity.

Figure 4 presents the optimum fits of some observed lifetime histograms of fibre composites and ceramics by the present theory and by the two-parameter Weibull distribution. Munz and Fett [32] conducted four-point-bend tests of the lifetime histograms of MgO-doped HPSN (hot-pressed silicon nitride) under constant stress at the temperature of 1100 °C and of 99.6% Al_2O_3 subjected to constant stress. The applied stress was about 50% of the mean short-time strength. Chiao *et al* [17] studied the lifetime distribution of organic fibre (Kevlar 49) composites. Bar-shaped specimens were subjected to constant uniform uniaxial tensile stress at elevated temperatures from 100 °C to 120 °C.

As seen in figure 4, the observed lifetime histograms plotted in Weibull scale do not appear as straight lines. Instead, there is a kink separating the entire histogram into two segments, of which the lower one is a straight line and the upper one deviates from it to the right. Similar deviations have also been found in the strength histograms of many other quasibrittle materials, such as concrete [45], fibre composite [40, 43] and ceramics [30, 34]. Clearly, the

two-parameter Weibull distribution cannot give optimum fits and the existence of the kink cannot be explained by it. In contrast, the present model gives an excellent fit of the entire lifetime histogram. In the present theory, the kink is caused by the finiteness of the number of links in the weakest link model and corresponds to the grafting point of the distribution, which reflects the quasibrittleness of the structure (and the non-locality of fracturing damage).

5. Size effect on lifetime distribution

From the finite weakest link model and the grafted cdf of lifetime for one RVE, it is clear that the type of lifetime cdf of structure must depend on the structure size and geometry. The mean lifetime can be easily evaluated as

$$\bar{\lambda} = \int_0^\infty [1 - P_f(\lambda)]\mathrm{d}\lambda. \tag{26}$$

Although a closed-form exact expression for $\bar{\lambda}$ is impossible, a good approximation can be obtained through the technique of asymptotic matching. This technique has been effectively used to describe the deterministic (or mean) size effect [6, 7, 12]. Since the random strength is related to the random lifetime through equation (19), the mean strength and lifetime must be related by an equation of the same form. Therefore, based on the approximate form of the deterministic size effect on structural strength [6, 13], the size effect on the mean structural lifetime can be written as [10]

$$\bar{\lambda} = \left[\frac{C_a}{D_s} + \left(\frac{C_b}{D_s}\right)^{r/m}\right]^{(n+1)/r}, \tag{27}$$

where m = Weibull modulus of strength distribution and n = exponent of crack growth law; $m/(n+1) = \bar{m}$ = Weibull modulus of lifetime distribution. Parameters C_a, C_b, r can be determined from three known asymptotic conditions for $[\bar{\lambda}]_{D_s\to l_0}$, $[\mathrm{d}\bar{\lambda}/\mathrm{d}D_s]_{D_s\to l_0}$, and $[\bar{\lambda}D_s^{1/\bar{m}}]_{D_s\to\infty}$. Figure 5 shows a typical size effect curve of structural lifetime. As seen, this size effect approaches, for large structure sizes, the power-law size effect of Weibull theory, but deviates from it upwards for small sizes, because of the finiteness of the FPZ.

6. Conclusions

This paper extends the previous work on the size (and shape) dependence of the probability distribution of structural strength [9, 11, 13, 14, 34] to the distribution of structural lifetime under constant load. The results may be summarized as follows

1. Fracture mechanics of random crack jumps in atomic lattice requires the subcritical crack growth rate to be proportional to the square of the stress intensity factor K (and to the Arrhenius temperature factor).
2. Based on the condition that the cumulative energy dissipation rate of all the nano-cracks must be equal to the macro-crack dissipation rate, the rise of the exponent of K from 2 to $n \approx 10$–30 during the nano–macro transition can be explained by considering that the number of active nano-cracks contained in the macro-scale FPZ must steeply increase with the applied macro-stress.

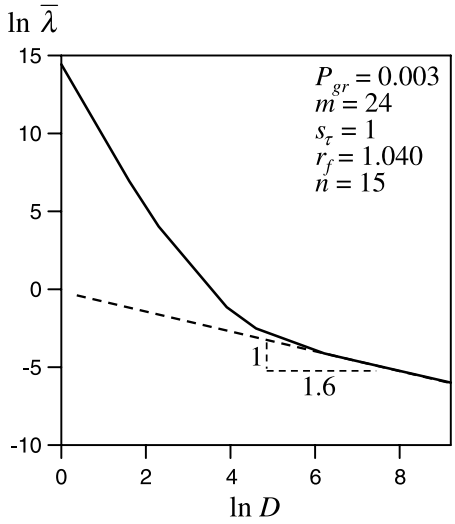

Figure 5. Curve of size effect on mean structural lifetime.

3. The crack growth rate law permits relating the probability distributions of strength and lifetime. This leads to a simple relation between the Weibull moduli of strength and lifetime (equation (25)), and permits deducing the lifetime distribution solely from the tests of (1) subcritical crack growth rate, and (2) strength histogram tests or the tests of size effect on structure strength (the latter being more efficient).
4. Like the strength distribution, the lifetime distribution of quasibrittle structures is found to vary with the structure size and geometry. A Weibull tail expands into the distribution core as the size increases. This is important for extrapolating small-scale or accelerated laboratory tests of lifetime to full-size real structures.

Acknowledgments

Partial financial supports under Grant CMS-0556323 from the US National Science Foundation and Grant N007613 from Boeing, Inc., both to Northwestern University, are gratefully appreciated.

References

[1] Alwis K G N C and Burgoyne C J 2004 Statistical lifetime prediction for aramid fibers *J. Compos. Constr.* **9** 106–16
[2] Aziz M J, Sabin P C and Lu G Q 1991 The activation strain tensor: nonhydrostatic stress effects on crystal growth kinetics *Phys. Rev.* B **41** 9812–16
[3] Barenblatt G I 2003 *Scaling* (Cambridge: Cambridge University Press)
[4] Barenblatt G I 1959 The formation of equilibrium cracks during brittle fracture, general ideas and hypothesis, axially symmetric cracks *Prikl. Mat. Mekh.* **23** 434–44
[5] Bažant Z P 1984 Size effect in blunt fracture: concrete, rock, metal *J. Eng. Mech. ASCE* **110** 518–35
[6] Bažant Z P 2004 Scaling theory of quasibrittle structural failure *Proc. Natl Acad. Sci. USA* **101** 13397–9
[7] Bažant Z P 2005 *Scaling of Structural Strength* 2nd edn (London: Elsevier)

[8] Bažant Z P and Chen E P 2007 Scaling of structural failure *Appl. Mech. Rev., ASME* **50** 593–627
[9] Bažant Z P, Le J-L and Bazant M Z 2008 Size effect on strength and lifetime distribution of quasibrittle structures implied by interatomic bond break activation *Proc. 17th Eur. Conf. on Fracture (Brno, Czech Republic)* pp 78–92
[10] Bažant Z P, Le J-L and Bazant M Z 2009 Scaling of strength and lifetime distribution of quasibrittle structures based on atomistic fracture mechanics *Proc. Natl Acad. Sci. USA* at press
[11] Bažant Z P and Le J-L 2009 Nano-mechanics based modeling of lifetime distribution of quasibrittle structures *J. Eng. Failure Anal.* at press
[12] Bažant Z P and Novák D 2000 Energetic-statistical size effect in quasibrittle failure at crack initiation *ACI Mater. J.* **97** 381–92
[13] Bažant Z P and Pang S-D 2006 Mechanics based statistics of failure risk of quasibrittle structures and size effect on safety factors *Proc. Natl Acad. Sci. USA* **103** 9434–9
[14] Bažant Z P and Pang S-D 2007 Activation energy based extreme value statistics and size effect in brittle and quasibrittle fracture *J. Mech. Phys. Solids* **55** 91–134
[15] Bažant Z P and Planas J 1998 *Fracture and Size Effect in Concrete and Other Quasibrittle Materials* (Boca Raton, FL: CRC Press)
[16] Bažant Z P and Prat P C 1988 Effect of temperature and humidity on fracture energy of concrete *ACI Mater. J.* **85-M32** 262–71
[17] Chiao C C, Sherry R J and Hetherington N W 1977 Experimental verification of an accelerated test for predicting the lifetime of organic fiber composites *J. Comput. Mater.* **11** 79–91
[18] Coleman B D 1957 Time dependence of mechanical breakdown in bundles of fibers: I. Constant total load *J. Appl. Phys.* **28** 1058–64
[19] Coleman B D 1958 Statitics and time dependence of mechanical breakdown in fibers *J. Appl. Phys.* **29** 968–83
[20] Duckett K 2005 Risk analysis and the acceptable probability of failure *Struct. Eng.* **83** 25–26
[21] Evans A G 1972 A method for evaluating the time-dependent failure characteristics of brittle materials—and its application to polycrystalline alumina *J. Mater. Sci.* **7** 1173–46
[22] Evans A G and Fu Y 1984 The mechanical behavior of alumina *Fracture in Ceramic Materials* (Park Ridge, NJ: Noyes Publications) pp 56–88
[23] Fett T 1991 A fracture-mechanical theory of subcritical crack growth in ceramics *Int. J. Fract.* **54** 117–30
[24] Fett T and Munz D 1991 Static and cyclic fatigue of ceramic materials *Ceramics Today—Tomorrow's Ceramics* ed P Vincenzini (Amsterdam: Elsevier) pp 1827–35
[25] Glasstone S, Laidler K J and Eyring H 1941 *The Theory of Rate Processes* (New York: McGraw-Hill)
[26] Hillig W B and Charles R J 1964 Surfaces, stress-dependent surface reaction, and strength *Proc. 2nd Berkeley Int. Materials Conf. (15–18 June)* ed V F Zackay
[27] Hsiao C C, Moghe S R and Kausch H H 1968 Time-dependent mechanical strength of oriented media *J. Appl. Phys.* **39** 3857–61
[28] Kaxiras E 2003 *Atomic and Electronic Structure of Solids* (Cambridge: Cambridge University Press)
[29] Krausz A S and Krausz K 1988 *Fracture Kinetics of Crack Growth* (Dordrecht: Kluwer)
[30] Le J-L and Bažant Z P 2009 Finite weakest link model with zero threshold for strength distribution of dental restorative ceramics *Dental Mater.* **25** 641–8
[31] Melchers R E 1987 *Structural Reliability, Analysis and Prediction* (New York: Wiley)
[32] Munz D and Fett T 1999*Ceramics: Mechanical Properties, Failure Behavior, Materials Selection* (Berlin: Springer)
[33] NKB (Nordic Committee for Building Structures) 1978 Recommendation for loading and safety regulations for structural design *NKB Report* No 36
[34] Pang S-D, Bažant Z P and Le J-L 2009 Statistics of strength of ceramics: finite weakest link model and necessity of zero threshold *Int. J. Frac.* (*Special Issue on Physical Aspects of Scaling*) **154** 131–45
[35] Philips R 2001 *Crystals, Defects and Microstructures: Modeling Across Scales* (Cambridge: Cambridge University Press)
[36] Phoenix S L 1978 The asymptotic time to failure of a mechanical system of parallel members *SIAM J. Appl. Math.* **34** 227–46
[37] Phoenix S L and Tierney L-J 1983 A statistical model for the time dependent failure of unidirectional composite materials under local elastic load-sharing among fibers *Eng. Fract. Mech.* **18** 193–215
[38] Redner S 2001 *A Guide to First-Passage Processes* (Cambridge: Cambridge University Press)
[39] Risken H 1989 *The Fokker–Plank Equation* 2nd edn (Berlin: Springer)
[40] Schwartz P 1987 A review of recent experimental results concerning the strength and time dependent behaviour of fibrous poly (paraphenylene terephthalamide) *Polym. Eng. Sci.* **27** 842–7
[41] Thouless M D, Hsueh C H and Evans A G 1983 A damage model of creep crack growth in polycrystals *Acta Metall.* **31** 1675–87
[42] Tobolsky A and Erying H 1943 Mechanical properties of polymeric materials *J. Chem. Phys.* **11** 125–34
[43] Wagner H D 1989 Stochastic concepts in the study of size effects in the mechanical strength of highly oriented polymeric materials *J. Polym. Sci.* **27** 115–49
[44] Wiederhorn S M 1967 Influence of water vapor on crack propagation in soda-lime glass *J. Am. Ceram. Soc.* **50** 407–14
[45] Weibull W 1939 The phenomenon of rupture in solids *Proc. R. Swedish Inst. Eng. Res.* (*Stockholm* 153) 1–55
[46] Zhurkov S N 1965 Kinetic concept of the strength of solids *Int. J. Fract. Mech.* **1** 311–23
[47] Zhurkov S N and Korsukov V E 1974 Atomic mechanism of fracture of solid polymer *J. Polym. Sci.* **12** 385–98